Electrochimica Acta 179 (2015) 441–451

Contents lists available at ScienceDirect

Electrochimica Acta

journal homepage: www.elsevier.com/locate/electacta

A New Strategy for Corrosion Inhibition Coatings for Lead Heritage Metal Objects

Victoria Flexer [a,1,*], Rosie Grayburn [a,b], Michel de Keersmaecker [a], Elbeshary A.A. Mohammed [a], Mark G. Dowsett [b], Annemie Adriaens [a,1]

[a] Department of Analytical Chemistry, Ghent University, Krijgslaan 281 (S12), Ghent 9000, Belgium
[b] Department of Physics, University of Warwick, Coventry CV4 7AL, UK

ARTICLE INFO

Article history:
Received 8 December 2014
Received in revised form 4 May 2015
Accepted 5 May 2015
Available online 6 May 2015

Keywords:
Lead
Cultural heritage
Corrosion resistance
Lead Carboxylate
Coating

ABSTRACT

Corrosion is the major problem in the degradation of heritage metal objects. The development of appropriate treatment methods to stabilize and protect artefacts is a undeniable scientific challenge. Here we propose a new coating method to protect lead heritage metal objects. This coating is environmentally safe, stable, reversible, easy to apply and to remove, and aesthetically justified. The coating consists of a compact and thick layer of lead ditetradecanoate, which is formed upon immersion of a lead substrate in a melted sample of tetradecanoic acid at 60 °C. Coated lead samples were exposed either to an aqueous corrosive environment or to a closed chamber with high relative humidity and an oak corrosive atmosphere. The corrosion resistance of the coating was followed for 60 days by electrochemical impedance spectroscopy and X-ray diffraction. Results show an unprecedented corrosion inhibition of the new coatings.

1. Introduction

Corrosion is the major problem in the degradation of heritage metal objects, and any remedial measures are subject to a strong ethic that favours conservation as opposed to restoration. Accordingly, major scientific challenges exist for developing appropriate treatment methods to stabilize and protect artefacts. Because inappropriate treatments can cause irreversible damage to unique and irreplaceable objects, it is crucial that the chemical processes involved are fully understood and characterized before any preservation work is undertaken. Besides being of fundamental interest, study of the corrosion behaviour is essential to the development of adequate conservation and preservation processes.[1,2]

It is common practice to protect metallic artefacts against corrosion using protective coatings.[2] Compared with industrial applications where the protective properties of the coating are the main parameter for their selection, when choosing coatings for heritage conservation treatments other properties should be considered[2,3]: i) visual appearance: coatings should be transparent; ii) reversibility: it should be possible to remove the coating and return the object to its original state; iii) respect the original object: treatments should not modify the material of the artefact; iv) long term efficiency and easy maintenance, since heritage artefacts are intended to be preserved for a long time. These considerations impose important limitations in the selection of corrosion inhibition coatings for this particular application.

Lead objects are ubiquitous amongst cultural heritage objects. Because of its low melting point and its malleability, lead was commonly used in ancient times.[4] Lead objects exposed to the atmosphere or buried usually corrode only slightly as the formation of a protective film, mainly of lead oxide and lead carbonates, drastically inhibits corrosion.[4,5] This explains why lead objects found at archaeological sites are usually in good condition. Conversely, lead corrodes severely in humid environments, specifically in the presence of organic acids vapours.[6,7] This accelerated degradation, commonly referred to as active corrosion, has become a serious issue in the case of historic organ pipes in churches or concert halls, since the pipes of ancient organs are made from lead, or lead-tin alloys.[8] In addition, lead archaeological objects have sometimes been kept for many years in wooden museum cases, often made of oak.[9] Earlier experiments have shown that a strong corrosion factor of pipe organ is the emission of organic acids in the air blown through the pipes.

* Corresponding author.
E-mail address: victoria.flexer@ugent.be (V. Flexer).
[1] ISE MEMBER

http://dx.doi.org/10.1016/j.electacta.2015.05.022
0013-4686/

[8]The organic acids are emitted from the wooden parts of the organ (in the windtrunks and in the windchests). Oak very often used in historic organs, as well as wooden museum cases, is known to emit large amounts of organic acids, especially acetic acid.[10] The application of a wax or acrylic coating has often been used to protect lead objects.[2,4] However these coatings are difficult to remove if further corrosion occurs, and failure of these coatings with severe damage to the original metallic object has been documented.[2] Lead corrosion has become an issue in recent years. New oak (instruments that underwent restoration), in a warmer and more humid environment (modern central heating systems) seems to be at the base of the problem.[6,8,11]

An effective and protective coating has been found in the use of coatings deposited from solutions of saturated linear monocarboxylates of the type $CH_3(CH_2)_{n-2}COONa$, hereafter noted C_nNa and C_n.[12,13] Rocca and Steinmetz showed that the protection is due to the growth of a crystalline lead monocarboxylate layer $[CH_3(CH_2)_{n-2}COO]_2Pb$ which passivates lead surfaces and inhibits corrosion, hereafter called $Pb(C_n)_2$. The degree of inhibition depends on the carbon chain length and on the carboxylate concentration in the solution used for coating: higher chain length and higher concentrations will result in higher effectiveness. [12,13] However, the solubility of both sodium carboxylates and the free carboxylic acids drastically decreases with increasing chain length, and therefore C chains longer than NaC_{12}/ C_{12} have hardly been investigated. Our group has further studied lead carboxylate coatings, with the aim of better characterizing the coatings and its relation with the corrosion resistance and to optimise the deposition method.[3,10,14–20] While these coatings produce a protective layer, the corrosion process is only slowed down, but not stopped. Therefore better coatings for the preservation of lead heritage metal objects are still much sought after.

Here we propose a new method for the formation of protective coatings for lead heritage objects. A coating with extremely high corrosion resistance qualities is spontaneously formed when a lead object is immersed in melted tetradecanoic acid, C_{14}. The resulting coating is a thick and compact layer of lead ditetradecanoate. The formation of such a coating is rendered possible because of the relatively low melting point of tetradecanoic acid. Electrochemical experiments clearly show the superior quality of this coating when compared to the classical micro-crystalline wax polish treatment currently in used by conservators. The time evolution of the Electrochemical Impedance Spectroscopy (EIS) signal shows that these coatings are stable over time. Moreover, time lapse EIS and X-ray diffraction experiments showed only minor evidence of corrosion products formation when lead coated samples were exposed for up to 59 days to a corrosive atmosphere.

2. Experimental

2.1. Chemicals

Tetradecanoic acid (C_{14}, myristic acid) was bought from SAFC, USA. The RENAISSANCE® micro-crystalline wax polish was a generous gift from Pricreator Renaissance Products, UK. All other chemicals were of Analytical grade.

The $Pb(C_{14})_2$ standard was prepared by precipitation, by mixing stoichiometric quantities of tetradecanoic acid and lead acetate, dissolved in the minimum possible amounts of ethanol and water, respectively. The precipitated product was washed three times with ethanol, and three times with water. It was dried in air, and characterized by elemental analysis, FT-IR spectroscopy and XRD.

2.2. Lead coupons preparation

Lead coupons were pressed from 2 mm thick 99.95% lead metal sheet (Goodfellow Ltd. Cambridge, UK) and machined in an oil-free environment to a diameter of 12.5 mm. One surface was then polished using a damp abrasive disc (BuehlerMet II) to remove visible surface defects and expose a fresh surface. Coupons were then polished using a sequence of polycrystalline diamond suspension (6 μm and 1 μm, Buehler MetaDi, 20 minutes each), rinsed with 2-propanol (99.5%, reagent grade) in between, and cleaned in 2-propanol for 5 min in an ultrasonic bath. Finally, the coupons were ultrasonically cleaned in 2-propanol for 3×5 min, with fresh propanol for each cleaning cycle.

Polished coupons were stored in 2-propanol for at least 30 days, and no longer than 50 days. These storage conditions were found to allow for the formation of a controlled lead oxide layer that forms spontaneously on any lead object upon exposure to air, thus allowing our simulant substrates to resemble more closely real lead objects.

2.3. Coating formation

Approximately 25 g of C_{14} were melted in a beaker in a laboratory oven at 60 °C (melting range for C_{14} is 52°-54 °C). The lead coupons were immersed in the melted C_{14} and left inside the oven at 60 °C for 18 hours. The coupons were removed from the molten acid, rinsed thoroughly in ethanol (3 rinsing steps of 20 mins each), and dried in air.

Another set of polished coupons was coated with a micro-crystalline wax polish. The wax was applied with a soft cloth. It was let to dry and harden for 1 hour and a clean cloth was used to gently buff the surface and remove the coarser pieces of wax.

The coating thickness was assessed by means of a coating thickness measuring gauge (CHECKLINE, DC FN-3000), which was calibrated by means of an uncoated sample. The coating thickness of 6 different $Pb(C_{14})_2$ coated coupons was measured. The thickness of each coupon was measured 20 times and all results were averaged. The coating thickness of the micro-crystalline wax polish was measured following a similar procedure.

For comparison, three coupons were also coated by immersion in an ethanolic solution of C_{14}, following the procedure reported by Grayburn *et al.*[10]

2.4. SEM measurements

Samples were sputter coated with C (Balzers Union Sputtering device). Scanning electron micrographs were recorded with a Phenom-FEI bench top scanning electron microscope (Phenom World BV, the Netherlands). Backscattered electrons (BSE) images were collected using 5 kV electrons and a solid state detector. Images were recorded in full mode (using the 4 quadrants of the detector) and in topography mode (using only 2 quadrants).

2.5. FT-IR experiments

FT-IR spectra were measured in the range 4400 to 600 nm in a Perkin-Elmer Spectrum1000 spectrometer equipped with a HATR (Horizontal Attenuated Total Reflection) cell from Pike Technologies. Spectra were measured on 3 different coupons and on 5 spots on each coupon. No differences were observed in between all these spectra.

2.6. X-ray diffraction experiments

To study long-term effects, an oak polluted environment was created within a 800 cm^3 desiccator. 150 cm^3 of a saturated

solution of NaCl at the base of the desiccator created an elevated relative humidity (RH): up to 75% for the ambient test temperatures ($20 \pm 3\,^{\circ}C$). Coated and uncoated lead samples were simultaneously placed on a shelf alongside ten $1\,cm^3$ oak cubes and four $4 \times 6 \times 1\,cm^3$ oak flat pieces within the desiccator for up to 59 days. The oak pieces were cut from a piece of contemporary oak (*Quercus sp.*) to expose a fresh oak surface. XRD measurements were performed using an ARL X'TRA diffractometer using Cu-Kα X-rays with a wavelength of .1540562 nm with a scintillation counter detector. A scan from 1 - 70° 2Θ was performed on each sample at a scan rate of 0.8°, 1° or 1.2°/minute and a step size of 0.02°. The spectra after 39 days of exposure on Fig. 10 was measured on a Siemens D5000 diffractometer under similar conditions. The XRD patterns were processed with our own software esaProject®2014. [21]

2.7. Electrochemical experiments

All electrochemical experiments were carried out in a three-electrode electrochemical glass cell with a carbon rod as a counter electrode and a saturated calomel electrode (SCE, Radiometer Analytical) as a reference electrode. Lead coupons were mounted in a homemade Teflon® working electrode holder. The ASTM D 1384–87 solution ($740\,mg\,L^{-1}$ Na_2SO_4, $690\,mg\,L^{-1}$ $NaHCO_3$, $825\,mg\,L^{-1}$ NaCl), was modified by the extra addition of $5\,mg\,L^{-1}$ acetic acid. All electrochemical experiments were performed in this solution, which models a typical atmospheric corrosive environment for lead (acetic acid in the reported concentrations around organ pipes and museum cases has been added to the standard electrolyte for corrosion inhibition tests). All electrochemical experiments were performed inside a Faraday cage.

Linear Sweep Voltammetry experiments were performed at a scan rate of $1\,mV\,s^{-1}$ on an AUTOLAB PGSTAT204 potentiostat. EIS measurements were performed on an AUTOLAB PGSTAT302N potentiostat equipped with a FRA2 frequency response analysis module. Data were acquired over a frequency range of 100 mHz to 10 kHz (0.01 V signal amplitude). The EIS measurements were carried out at the open circuit potential, which was measured before each EIS scan, until a constant value with a variation of $0.1\,\mu Vs^{-1}$ or less was reached. The frequency range was distributed logarithmically. Experiments were controlled by the Nova software (version 1.10, Ecochemie, The Netherlands). The same software was used to perform Impedance fitting analysis to the corresponding equivalent circuits.

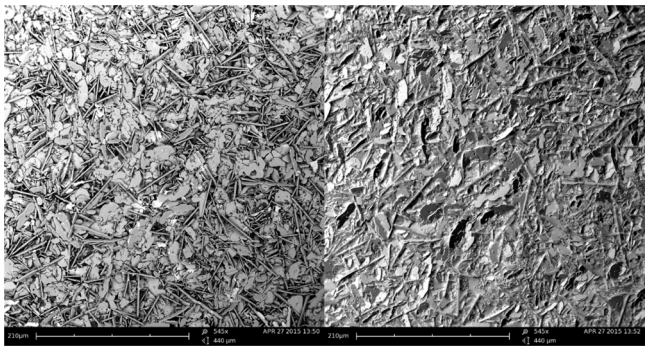

Fig. 1. SEM micrographs of a $Pb(C_{14})_2$ coated sample. Left: full image (full detector in use). Right: topographic image.

Every type of electrode was measured in triplicate. Results reported here were in very good agreement with the corresponding replicates with regards to the shape of the curves (both LSV and EIS), and the order of magnitude of the respective signals. The precise curves differ slightly in magnitude values from replicate to replicate. Differences are attributed to two factors: 1-the soft nature of lead renders the reproduction of the initial surface very difficult, despite careful polishing; 2-both coating methods still need improvement for precise control of the coating thickness layer.

3. Results and Discussion

3.1. Characterization of the coating

Tetradecanoic acid, C_{14}, was originally chosen as a candidate for coating formation as it is the first long chain carboxylic acid which is completely insoluble in water in either the acid or the salt form.

The coating thickness was estimated at (27 ± 6) μm. The dispersion in thickness values suggests that the coating formation protocol is not yet fully optimized. Fig. 1 *a* shows an SEM image of the coating, depicting medium size crystals, with some preferential orientation. In Fig. 1 *b* the coating seems to be very compact.

The coating formation was assessed by means of both FT-IR spectroscopy and X-ray diffraction, comparing the spectra of the coated surface to reference powder spectra. Fig. 2 shows an FT-IR spectrum of the coating (thick line) compared to the spectra of both standard C_{14}, and $Pb(C_{14})_2$. The spectrum of the coating bares

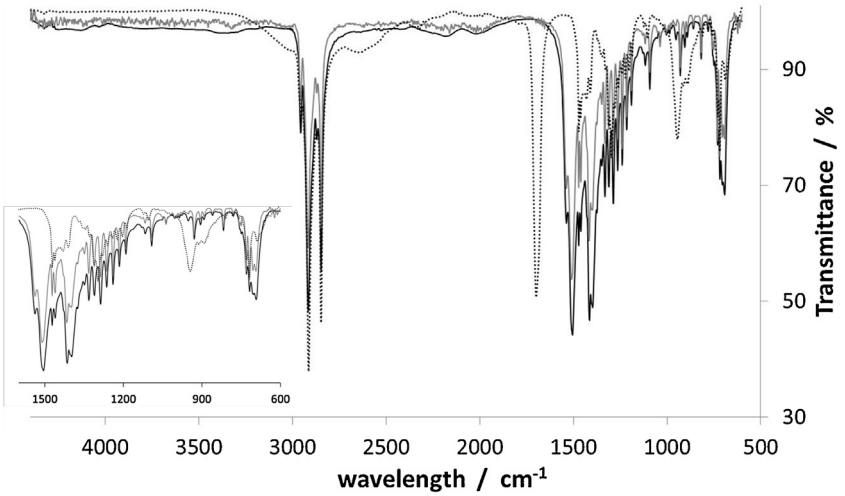

Fig. 2. FT-IR spectra of melted tetradecanoic acid coated lead coupon (black solid line). The spectra of the standards for tetradecanoic acid (black dotted line) and $Pb(C_{14})_2$ (grey solid line) are also plotted for comparison. Inset: zoom in the fingerprint region.

a strong similarity to the spectra of the lead tetradecanoate standard, suggesting the successful formation of a lead tetradecanoate layer. The band observed at 1510 cm^{-1} is identified as the antisymmetric mode, ν_a COO^-. The band at 1416 cm^{-1} is the symmetric stretching mode, ν_s, COO^-.[19] These two bands appear as doublets characteristic of long chain bivalent metal carboxylates.[22,23] Finally the band at 930 cm^{-1}, ν_d, is identified as the deformation band COO^-.[19] Moreover, the spectrum does not show any of the characteristic peaks of C_{14}, which leads us to discard the idea of unreacted acid remaining as part of the coating. There is no trace in the spectra of the coating of the band at 1698 cm^{-1}, which is very strong in the unreacted tetradecanoic acid and represents the OH^- stretching. The remaining peaks in the fingerprint region are also distinctly different in the unreacted acid and in the coating.

If the coupons are not rinsed in ethanol after the overnight reaction in C_{14}, the FT-IR and the XRD indicate the presence of both $Pb(C_{14})_2$, and unreacted acid, C_{14}. After the coupons are rinsed in ethanol, only the signal of $Pb(C_{14})_2$ is observed. This is because the C_{14} molecules have a high solubility in ethanol, whereas the lead carboxylate is insoluble in ethanol.[10]

Fig. 3 shows the X-ray diffraction pattern of a coated coupon. It is straightforward to assign the five peaks corresponding to the underlying lead substrate (see labelling in Fig. 3). Unfortunately, to the best of our knowledge, there is no high quality reference pattern for lead tetradecanoate (the presumed compound in our coating) for comparison with our own pattern. Our XRD pattern shows however a very high similarity to the International Centre for Diffraction Database, ICDD, reference number 00-049-1964, and to the high quality powder pattern previously reported by Grayburn *et al.*[10] We can clearly distinguish the even reflexions in the series 002, 004, . . . ,0018. These peaks show the characteristic uniform spacing of 1.56 nm^{-1}, and are labelled in Fig. 3.[10] Comparison with these previously published spectra confirms that the coating consist mainly of $Pb(C_{14})_2$.

There are still 4 rather intense peaks, marked with an asterisk, which were not associated to $Pb(C_{14})_2$ before. Because of the simplicity of the coating deposition strategy, there is not a large number of compounds that could potentially be formed and detected by XRD. The only candidate products are: 1- corrosion products (due to an accelerated corrosion process at high temperature); 2- C_{14} decomposition products (during heating); 3-unreacted C_{14} (free acid). We discard the first hypothesis, since those peaks do not fit with any of the known lead corrosion products.[10] Hypothesis 2 and 3, are not compatible with the FT-IR evidence that did not show any bands different from the ones in the standard $Pb(C_{14})_2$.

The first two unassigned peaks are also observable in some of spectra by Grayburn *et al.*[10] The difference in relative intensity for those peaks could possibly be related to preferential orientation of the $Pb(C_{14})_2$ crystals following different formation mechanisms. Moreover, our diffractograms bare a very strong qualitatively similarity to ICDD references 00-009-0712 and 00-005-0332 for $Pb(C_{10})_2$ and lead $Pb(C_{12})_2$, respectively. Peaks very similar to all 4 unassigned peaks are present in those patterns. Those reference patterns are also of low quality, therefore with certain limitations, but unlike the $Pb(C_{14})_2$ pattern, they have been recorded to higher Q. Those signals seem to be related to the head group of the lead carboxylate (PbCOO). Although the structures for $Pb(C_n)_2$ compounds have never been solved beyond $Pb(C_7)_2$[24], it is to be expected that they present very similar crystallization patterns, notably, in the plane where the lead carboxylate groups lie, with similar plane spacings regardless of the carboxylate chain length. In conclusion, those 4 large peaks are most probably attributable to the $Pb(C_{14})_2$ structure, and we can conclude that the coating is only composed of this compound.

3.2. Protective nature of the coating

3.2.1. Electrochemical Experiments

In order to evaluate the protective properties of the new coating, its behaviour in corrosive media was compared to the behaviour of both uncoated coupons (*i.e.* protected only by the naturally forming PbO layer[4]) and by coupons coated with a micro-crystalline wax polish.[2,4]

Fig. 4 shows the linear sweep voltammograms in corrosive media for a coupon coated by our new proposed method, and an uncoated coupon. It can be observed that both the anodic and cathodic currents for the coated electrode are about two orders of magnitude lower than in the case of the uncoated electrode.

Although a precise calculation of the Tafel slope seems rather difficult from our LSV curves, it is evident that the coated electrode shows a much lower anodic Tafel slope as compared to the uncoated electrode. This decrease can be associated with both anodic and cathodic effects on the corrosion mechanism. $Pb(C_{14})_2$ is acting as a strong corrosion inhibitor, by delaying the oxidation and the

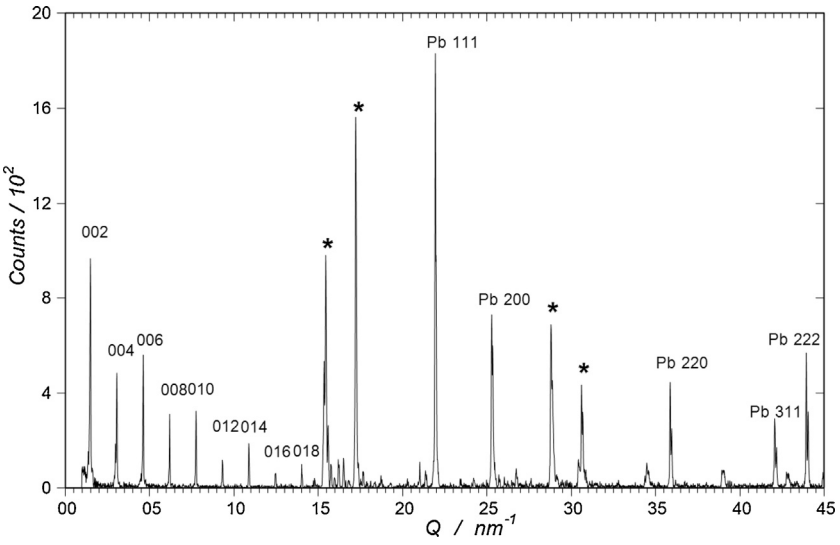

Fig. 3. XRD pattern of a melted tetradecanoic acid coated lead coupon on a freshly prepared sample. The assignment of the peaks is discussed in the text.

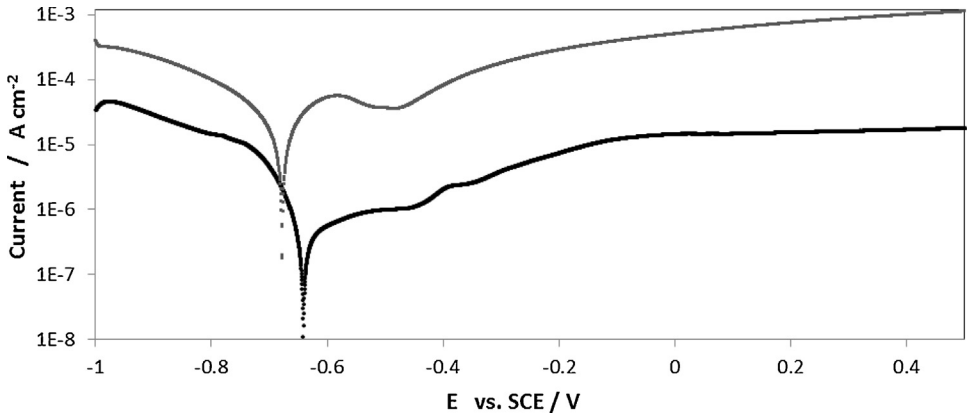

Fig. 4. Linear sweep voltammogram of a $Pb(C_{14})_2$ coated electrode (black) and an uncoated lead electrode (grey). Scan rate 1 mV s^{-1}. Electrodes soaked in the corrosive media for 30 minutes prior to scan.

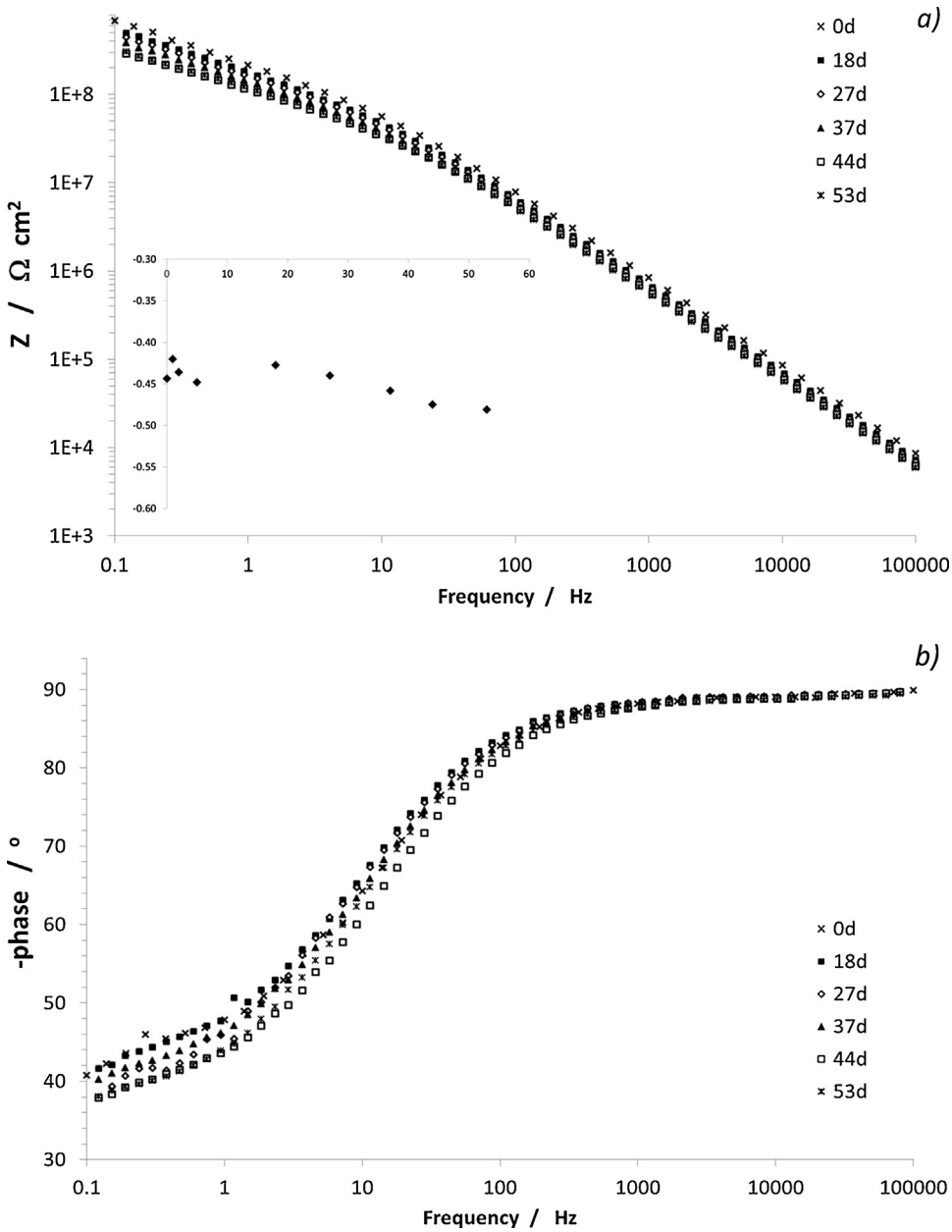

Fig. 5. Time evolution of EIS Bode modulus (*a*) and phase angle (*b*) plots obtained for a $Pb(C_{14})_2$ coated coupon during immersion in corrosive media. Elapsed time as indicated in the. Inset in (*a*): evolution of the corrosion potential during immersion (in V vs. SCE).

dissolution of metallic lead. The decrease in cathodic and anodic currents with respect to the uncoated electrode is observed for the entire scanned potential window, which suggests very good barrier properties and indicates that the passivation mechanism is effective not only around E_{corr}, but for all the potential range under study. This is a very encouraging result, particularly when compared to previous work with shorter chain carboxylate coatings prepared from aqueous solutions. In those studies, the passivation had only been observed up to about -200 mV.[16] The marked decrease in current strongly suggests that the $Pb(C_{14})_2$ coating forms a very stable film blocking a great majority of the anodic and cathodic sites on the metallic lead surface. Moreover, we observe a shift towards more noble potentials of E_{corr}. This shift is probably associated with a change in the corrosion mechanism forced by the blocking of most of the metallic surface by the protective coating.

In order to assess the long term response of the coating in corrosive media, two different exposure experiments were designed. In the first one, lead coupons coated with the new coating, the classical micro-crystalline wax polish and uncoated coupons were left immersed in a corrosive solution and Electrochemical Impedance Spectroscopy experiments were performed in the same solutions at regular intervals for periods of up to 53 days.

Fig. 5 shows the time evolution of the impedance magnitude values (*a*) and phase angle shifts (*b*) for the new coating. For comparison, the time evolution of the same variables are shown for an uncoated coupon in Fig. 6 (*a*) and (*b*), and for a micro-crystalline wax coated coupon (*c*). Not all the experiments performed are shown in Fig. 5 since during the first 2 weeks of exposure no visible changes were observed in the Bode plots.

In Fig. 5, we observe first that there are only very small visible changes in the Bode plots of the $Pb(C_{14})_2$ coated coupons. During the 53 days, the magnitude of the impedance at low frequency only decreased from $5.8 \times 10^8\,\Omega\,cm^{-2}$ to $3.0 \times 10^8\,\Omega\,cm^{-2}$. This is an extremely good result if we consider that the electrodes were constantly immersed in the corrosive media. On the other hand, the phase angle plot only shifted slightly, while keeping the overall shape of the curve. The shape of the Bode plots shows the characteristic response of a capacitor, with an almost constant -90° phase shift at high and mid-frequencies, and a high pore resistance as the electrolyte very slowly penetrates the coating. [2,25] The time evolution of the corrosion potential, shown in the inset in Fig. 5 (*a*), shows only a very small variation with time, in agreement with the stability observed in the Bode plots.

The shape and the time evolution of the Bode plots are distinctly different in the case of the uncoated and the micro-crystalline wax coated coupons when compared with the $Pb(C_{14})_2$ coated samples. We observe first that at time zero, the coupons with a $Pb(C_{14})_2$ coating show impedance magnitude values, that are 3 orders of magnitude higher than those for the micro-crystalline wax coated coupons and 4 orders of magnitude higher than the uncoated coupons. Moreover, the shape of the phase angle plots shown in Fig. 6 are distinctly different from the flat -90° behaviour shown by the $Pb(C_{14})_2$ coated samples. The plots in Figs. 6 (*b*) and (*c*) are characteristic of a partially permeable coating that allows corrosion to some extent.[2,25] The uncoated lead electrode is only protected against further corrosion by the native PbO oxide layer. As observed in Fig. 6, upon exposure to a corrosive media for just a few hours, the Bode plots changed considerably, the impedance magnitude value increases and the capacitive response in the phase angle plot also increases and becomes broader. This behaviour suggests that important changes at surface level are occurring to this electrode, *i.e.* that a corrosion process is taking place. We interpret these changes as the deposition of insoluble oxidation products on the electrode surface, of which the first apparent effect is protection. Further corrosion is slowed down because of the presence of these corrosion products at the

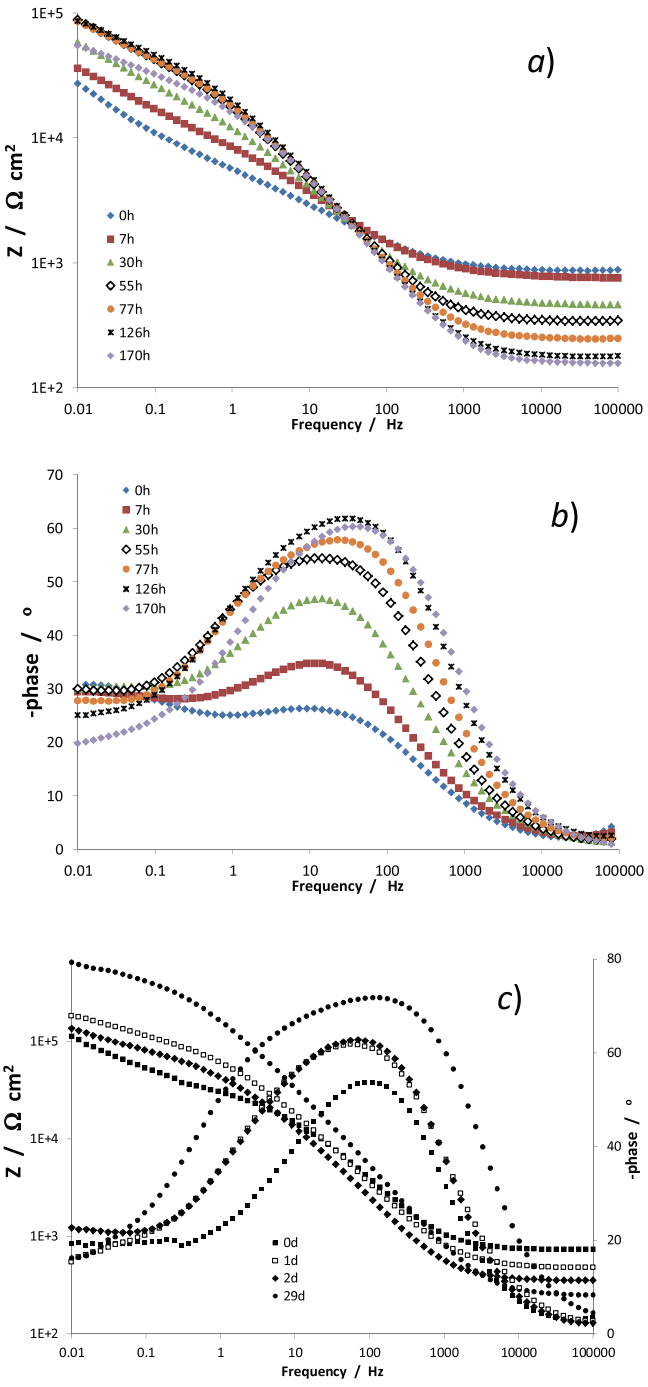

Fig. 6. Time evolution of EIS Bode modulus (*a*) and phase angle (*b*) plots for an uncoated lead coupon immersed in corrosive media. Time evolution of EIS Bode modulus and phase angle plots (*c*) for a micro-crystalline wax coated coupon immersed in corrosive media. Elapsed time as indicated in the. Markers in colour in the online version.

electrode surface, making it more difficult for the aggressive species to come in contact with the metallic lead. The changes are fastest during the first 3 days of the exposure experiment, when changes in the Bode plots were recorded every 2 hours (for visual clarity, not all these curves are shown in Fig. 6). After 3 days, the changes slow down, with the impedance magnitude values at low frequencies remaining approximately constant. The capacitive loop in the mid-frequency range continues to broaden slowly, while changes are also observed at high frequencies for the impedance magnitude values. After about 1 week of exposure, the

impedance magnitude values start to decrease. This might suggest that despite the slight protective effect of the insoluble corrosion products, the metallic lead slowly starts to form soluble corrosion products.

The changes in the Bode plots for the micro-crystalline wax coated coupons are not as fast as those observed in the uncoated coupons, as expected from a partially protective coating. Note that Figs. 6 (*a*) and (*b*) depict changes over only 1 week, while Fig.6 (*c*) depicts changes over a month. Albeit at a much slower rate, a similar trend as that observed in the uncoated coupon is recorded here, with increases in both the impedance magnitude values and the capacitive behaviour at intermediate frequencies. Most likely, these changes are associated with a similar corrosion mechanism, and with an initial deposition on the surface of insoluble corrosion products, which partially protect the metallic surface, slowing down, but not completely stopping the corrosion process.

A more quantitative interpretation of the EIS results is achieved for the $Pb(C_{14})_2$ coated and uncoated coupons by numerical fitting the experimental data to the equivalent circuits depicted in Figs. 7 *a* and *b* respectively. While data from the $Pb(C_{14})_2$ coated samples were fitted to a circuit depicting 2 time constants, data from the uncoated samples were fitted to a circuit with three time constants. For the equivalent circuit shown in Fig. 7 *a*, R_U is interpreted as the resistance of the electrolyte; $C_{coating}$ and $R_{coating}$ represent, respectively, the capacitance and the resistance (resistance associated to the pores) of the coating. CPE_{DL} is a constant phase element associated to the capacitance of the electrochemical double layer at the metal/coating interface; and R_{CT} is the charge transfer resistance of the metal. For the equivalent circuit depicted in Fig. 7 *b*, R_U, CPE_{DL} and R_{CT} are interpreted in the same way as for the previous circuit. $R_{coating}$ and $CPE_{coating}$ are similar as above, except they refer to the native oxide layer, PbO on top of the metallic surface. Finally, as previously suggested,[16] C_{PART} and R_{PART} are attributed to an extra resistance originating in particles left behind by the polishing step (particles which are probably removed during coating formation). In these equivalent circuits, some constant phase elements (CPE) were used instead of pure capacitors, because of the non-ideal character of the corresponding responses. This is due to roughness that arises from both the underlying lead metal surface, the $Pb(C_{14})_2$ coating, or the native oxide layer, PbO, which gives rise to certain surface inhomogeneities. The true capacitance can be calculated from the respective CPE parameters, as described elsewhere.[26–28] The variation of the fitted parameters with immersion time using the equivalent circuits from Fig. 7 are shown in Figs. 8 and 9 for the $Pb(C_{14})_2$ coated and the uncoated samples respectively, and are also listed in Tables S1 and S2 in Supporting Information. The fittings are in good agreement with the experimental data for all the samples. Values are shown with the errors from the numerical fitting, although these are most of the time below 5% and hence indistinguishable in the plots.

In the case of the $Pb(C_{14})_2$ coated sample, the $C_{coating}$ slowly increases with time, while the respective $R_{coating}$ slowly decreases. These changes can be considered minor, capacitance coating values in the order of 10^{-10} F cm^{-2} and coating resistances in the order of $10^7\ \Omega$ cm^{-2} are usually associated with excellent coating capabilities.[27] The rather small changes in $C_{coating}$ suggest very low water permeation of the coating and a negligible degree of delamination. We can also appreciate that the error associated to the fitting of this passive element is the lowest of all the fitting parameters, and is therefore one of the most effective parameters to assess coating behaviour, as previously observed.[29] The order of magnitude of the $R_{coating}$ values suggests that the coating is not really porous, but rather that the electrolyte might penetrate only in between Pb $(C_{14})_2$ crystalline grain boundaries. These high values are also most probably associated to the high thickness of these coatings.

The values of the Y_{DL} constant from the CPE_{DL} are also very low, and only increase slightly with time. The n value of this CPE element kept constant in time, at a value of 0.63. Likewise, the R_{CT} is very high and only decreases slightly with time. These values suggest that only a very small fraction of the metallic surface area is available for double layer formation, and potential corrosion reactions to take place. Moreover, they correlate with an extremely low corrosion current, as previously observed in the LSV.

For the uncoated sample, the analysis of the fitting of the EIS data to the corresponding equivalent circuit shows in the first place quite sharp variations with time. The fittings at time zero are in good agreement with previously published results for uncoated Pb. [16] The resistance attributed to the particle layer decreases quite sharply during the first two days. During the same time interval, the capacitance associated with those same particles changes abruptly, which we can possibly attribute to the removal of some of these particles with the dissolution of metallic lead and/or the formation of corrosion products. The resistance associated to the

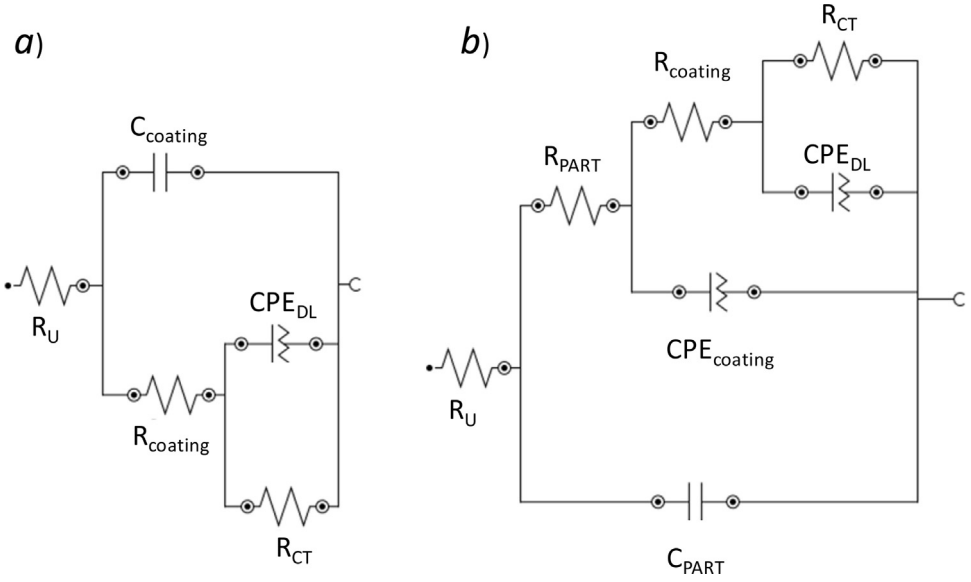

Fig. 7. Equivalent circuits used for the numerical fitting of EIS data for the $Pb(C_{14})_2$ coated (*a*), and uncoated (*b*) coupons during immersion in corrosive media.

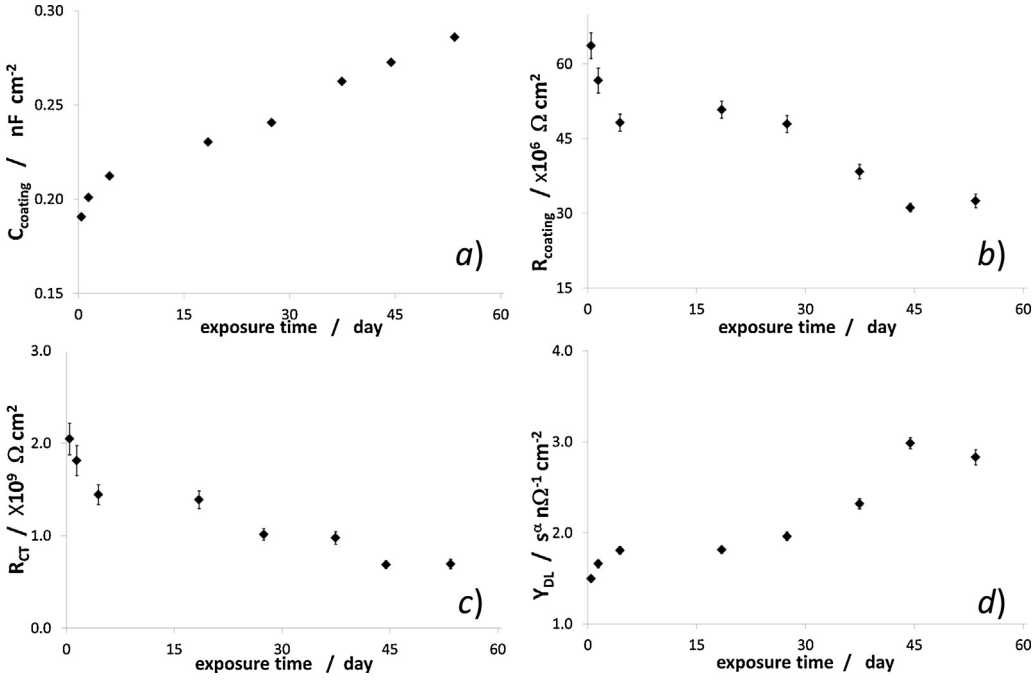

Fig. 8. Time evolution of the coating capacitance (*a*); coating resistance (*b*); charge transfer resistance (*c*); and double layer CPE constant (*d*) for a $Pb(C_{14})_2$ coated coupon upon immersion in corrosive media.

PbO native layer and the resistance to charge transfer follow very similar trends. They increase during the first hours of exposure, arrive at a maximum value and then they decrease steadily. A complementary trend is observed for the Y constants from the CPE elements. These values decrease during the first hours and then they remain, on average, constant. The corresponding α exponents vary with time, as depicted in the insets of Fig. 9 (*d*) and (*f*). The α values close to 0.5 are an indication of important diffusional components, rather than pure capacitors, hence, probably pointing to the ongoing corrosion reactions been limited either by diffusion from reactants towards or products out of the electrode surface.

Finally, for those circuit elements that can be compared between the two coatings (R_{CT}, Y_{DL}, $R_{coating}$), we observe large differences in fitted values from the $Pb(C_{14})_2$ coating to the uncoated coupons (PbO native layer). These variations are simply a correlation of the differences observed in the original Bode plots.

3.2.2. Exposure to an oak vapours rich atmosphere

The second long time exposure experiment is summarized in Figs. 10 and 11. Fig. 10 shows the diffraction patterns for five $Pb(C_{14})_2$ coated coupons unexposed and exposed to an oak and humid environment for different periods. Each pattern corresponds to a different coupon: coupons were simultaneously introduced in the chamber, and extracted one at a time to allow for different exposures. These experiments were performed for assessing the potential appearance of crystalline corrosion products, and the degradation of the coating. The y-axis of the XRD patterns are shown in a square root scale to highlight peaks of lower intensity. The patterns were measured at different scan rates, which partially accounts for the varying integrations of the same peaks in the different diffractograms. Moreover, the coating method might not yet be fully optimised with regards to homogeneous coating thickness. Therefore, a quantitative comparison of the peak intensities should be carried out with care. The patterns are useful for a qualitative comparison, *i.e.* presence or not of the different peaks.

The most important feature we observe by comparing the five patterns, is that hardly any new peaks develops during the exposure experiments. This is a strong indication of the good barrier properties of the coating and of its protective nature. This is in clear contrast to the results obtained with both the uncoated coupons and the micro-crystalline wax coated coupons (see Fig. 11), where corrosion products are clearly visible after only 22 days of exposure to exactly the same environment.

It can be observed that all the peaks in the first pattern (unexposed to the oak environment) are still present in the four consecutive patterns. These peaks have previously been attributed to either the underlying lead substrate or the $Pb(C_{14})_2$. The relative intensities of the lead and $Pb(C_{14})_2$ peaks vary from pattern to pattern. This is most probably attributable to variations in coating thickness, rather than degradation of the coating (the $Pb(C_{14})_2$ peaks become more intense than the lead peaks for the last patterns). Some peaks that were barely distinguishable in Fig. 3 are now clearer in the topmost pattern (unexposed to oak) because of the square root scale in the y axis. As discussed in section 3.1, most of the low intensity peaks between Q = 15.0 and 34.0 nm^{-1} are likely to belong to $Pb(C_{14})_2$. The small peaks at Q = 38.9 and 42.8 nm^{-1} have been attributed to hydrocerussite [$Pb_3(CO_3)_2(OH)_2$, syn], and plumbonacrite [$6PbCO_3.3Pb(OH)_2.PbO$], respectively. We did not find a matching reference for the peak at 34.5 nm^{-1}. Lead carbonate compounds have been reported as spontaneously forming passivating layers.[4] However, these corrosion products seem to be forming during the heating process, since they are not visible in the unexposed coupons that did not undergo heat exposure (see topmost patterns in Fig. 11). While the formation of these corrosion products is undesired, the fact that the relative intensity of these peaks remains mostly unchanged in the next diffractograms suggests that they have passivated the lead surface and are not associated to active corrosion processes. Small peaks assigned to β-lead oxide (massicot), plumbonacrite and hydrocerussite appear in the last diffractogram. All the reference XRD patterns are listed in the caption of Fig. 11.

Fig. 11 (*a*) shows two diffraction patterns of uncoated coupons exposed to the oak environment and are compared to the pattern of an unexposed coupon. The top pattern shows the classical pattern of a lead substrate, and some peaks of lower intensity that

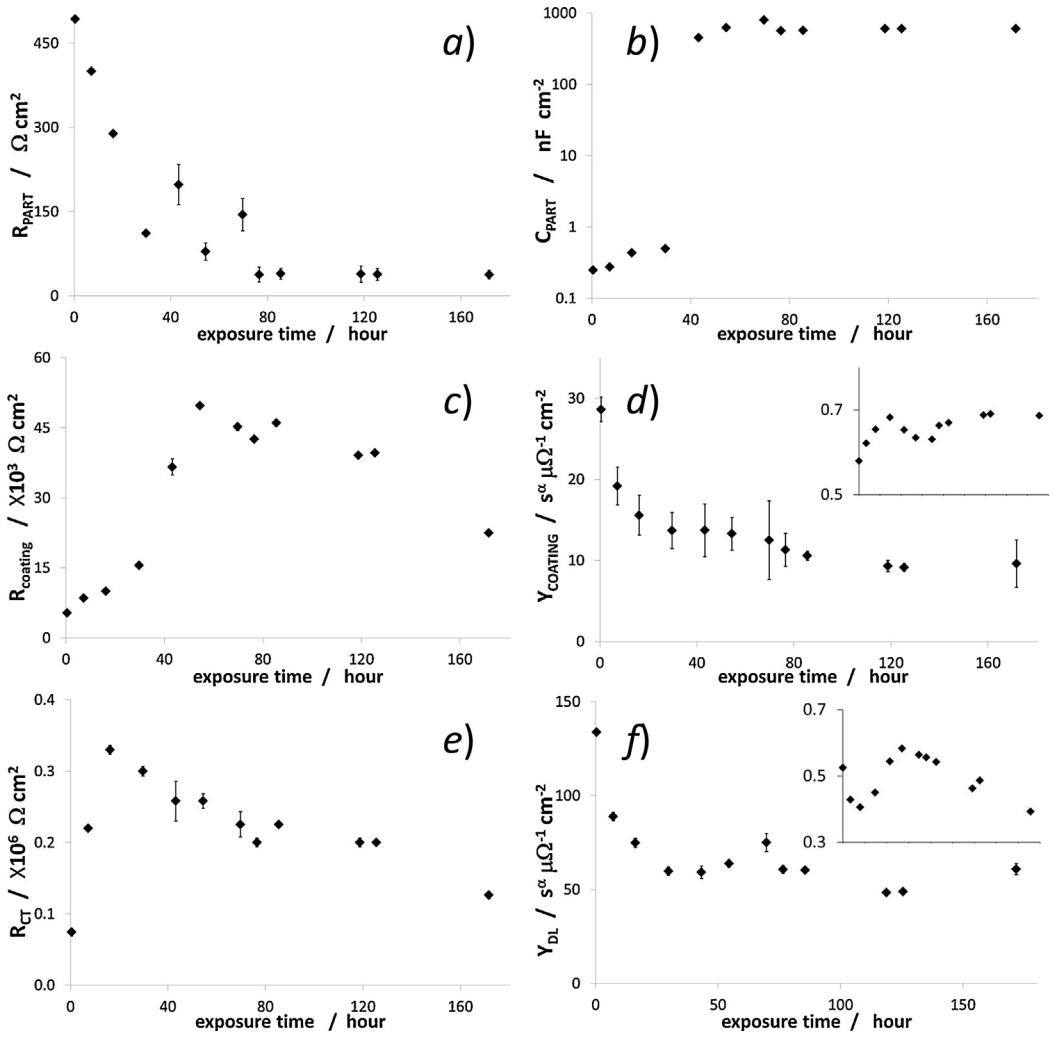

Fig. 9. Time evolution of the particle layer resistance (*a*); particle layer capacitance (*b*) PbO coating resistance (*c*); PbO layer CPE constant (*d*); charge transfer resistance (*e*); and double layer CPE constant (*f*) for an uncoated Pb coupon upon immersion in corrosive media. Insets in (*d*) and (*f*) correspond to the time evolution of the corresponding α exponents of the CPE elements.

have been assigned to β-lead oxide (massicot) and hydrocerussite. These corrosion products were formed during the storage time of the coupons (see Experimental section). After 29 days of exposure, more than 10 peaks that were not present in the diffractograms of the unexposed coupon are already observable. These peaks have been assigned to lead oxide (β-PbO-massicot), hydrocerussite [$Pb_3(CO_3)_2(OH)_2$, in both syn and trig crystalline structures], plumbonacrite [$6PbCO_3.3Pb(OH)_2.PbO$], lead acetate oxide hydrate [$Pb_3(CH_3COO)_6.PbO.H_2O$], and lead formate [$Pb(HCO_2)_2$], as marked in the figure. All these compounds are classical lead corrosion products in the presence of volatile organic compounds emitted from oak.[10] After 49 days, even more peaks from corrosion products are apparent in the diffractogram, while the intensity of the peaks that were already present in the previous pattern (29 days) has considerably increased.

Finally, Fig. 11 (*b*) shows the diffraction patterns for 2 micro-crystalline wax coated coupons exposed to the humid oak environment and the pattern of an unexposed coupon. The latter shows the 5 peaks corresponding to the underlying lead substrate. The remaining peaks, of much less intensity, have been assigned to β-lead oxide (massicot) and hydrocerussite. After only 22 days of exposure, already eight new peaks appear in the pattern. These peaks have been assigned to lead oxide, hydrocerussite, plumbonacrite, and lead formate, as marked in the figure. After 40 days, those corrosion peaks more than double their intensity in comparison to the lead peaks, evidencing an ongoing corrosion process. Also, some new peaks are evident, notably with the appearance of lead acetate oxide hydrate and the remaining assigned to the same compounds observed after 22 days.

Finally, a visual comparison of the as prepared coupons and coupons exposed to the oak rich environment shows that the visual appearance of the new coating is unaltered, while both the uncoated and micro-crystalline wax coated coupons show the characteristic white traces of lead corrosion (see Fig. S1 in S. I.)

3.2.3. Comparison

The XRD patterns following the exposure tests are in very good agreement with the results from the EIS tests. The EIS tests after exposure in aqueous corrosive media, suggested that the $Pb(C_{14})_2$ coating was very stable and that no corrosion layer was being developed. This is essentially the same information that is extracted from the XRD patterns. On the other hand, both in the case of the uncoated coupon and the micro-crystalline wax coated coupons, the EIS suggested that a corrosion layer was being formed during the exposure experiments in corrosive aqueous media. In parallel, the XRD patterns showed the formation to a large extent of

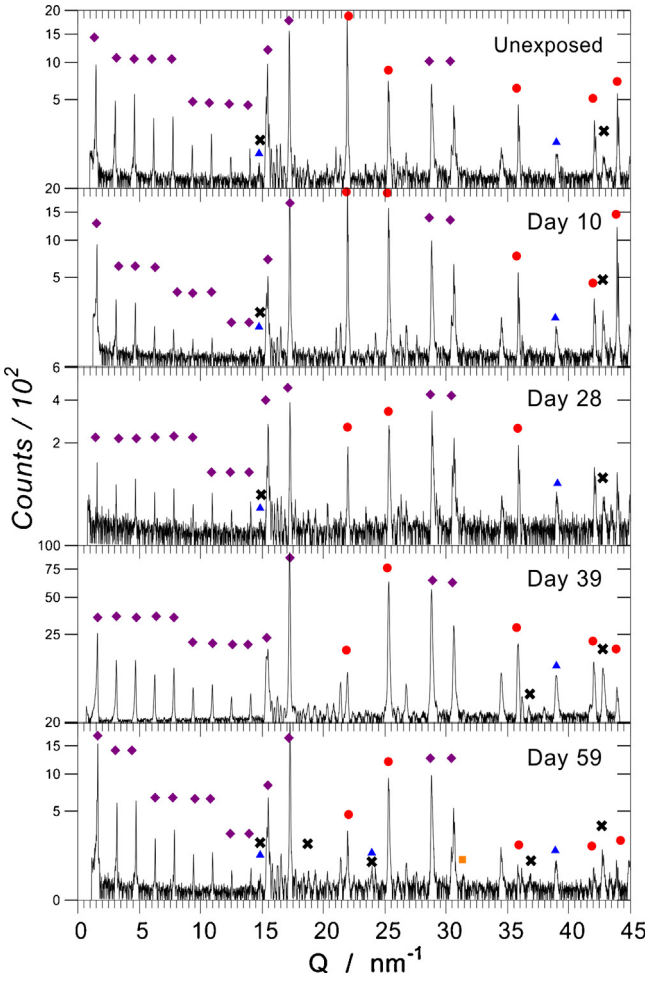

Fig. 10. XRD patterns of $Pb(C_{14})_2$ coated coupons after different exposure times in a humid oak environment. Suggested peak assignment according to references as specified in the caption of Fig. 11. Markers in colour in the online version.

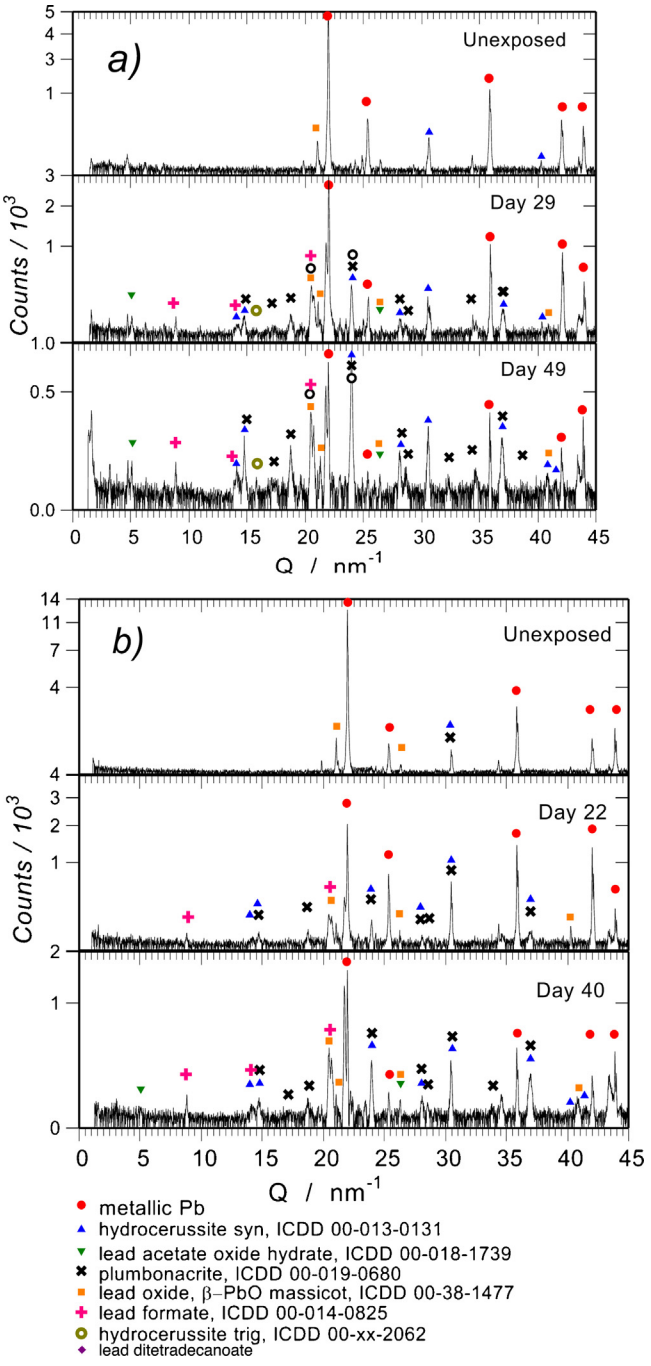

Fig. 11. XRD patterns of uncoated lead coupons (*a*), and microcristaline-wax coated lead coupons (*b*) after different exposure times in a humid oak environment. Suggested peak assignment according to references as specified in the figure caption. Markers in colour in the online version.

several corrosion products. Both for the EIS and for the XRD experiments, the corrosion rate was much faster for the uncoated coupons than for the micro-crystalline wax coated coupons.

These experiments prove that despite their wide use by conservators all over Europe, the micro-crystalline wax is not a completely efficient coating for the protection of lead objects. Our new proposed coatings seem to be much more efficient in preventing corrosion.

The barrier properties and the protective nature against corrosion of our new proposed coating method seems to be by far the most efficient from all lead carboxylate coatings reported so far. Indeed, $Pb(C_{14})_2$ and lead dioctadecanoate coatings prepared from ethanolic solutions of the free acid showed impedance magnitude values 4 orders of magnitude lower[20] than reported here, while similar exposure tests to a corrosive atmosphere showed a much larger extent of ongoing corrosion than reported here.[10]

Coatings prepared from aqueous solutions of sodium decanoate and dodecanoate showed impedance magnitude values at low frequencies ranging between 2 and 5 orders of magnitude lower than reported here. Moreover the phase angle plots did not show the characteristic behaviour of a capacitor shown by our coatings.[3,14–16,18] Although the corrosion inhibition properties were assessed by different methods, our coatings also seem to be more efficient than the original work on lead carboxylates reported by Rocca *et al.*[12,13] In that work, Rocca *et al.* arrived at the conclusion that both longer chain carboxylates and increased concentrations in the coating solutions would produce more protective coatings.[13] We believe that the strong enhancement in the corrosion resistance of our coatings is not only due to the longer chain lengths (C_{14}, vs C_{12}, C_{11}, C_{10} in most of the work previously reported), but most importantly to a thicker and more dense coating layer. Indeed, the fact that the lead carboxylate layer is formed in a much higher concentration of carboxylate moieties (pure molten acid) seems likely to accelerate the formation of lead carboxylate. We have measured the coating thickness of coupons prepared following immersion in ethanolic solutions of

tetradecanoic acid to be (5 ± 3) μm. If we recall that our method yields coatings of 6 times this thickness value, (27 ± 6) μm, it is therefore reasonable to observe the results reported here regarding the resistance of the coatings. These thicker coatings are likely to provide better barrier properties against the attack of aggressive species, most notably acetic acid. This high thickness value is most probably the reason behind the almost perfect capacitive behaviour in the Bode plots. For comparison, thickness measurements for the micro-crystalline wax coated coupons yielded a value of (6 ± 4)μm. Because of the different chemical nature of the coating, we cannot fully attribute the lower protection of micro-crystalline wax coating to its lower thickness. However, the difference in thickness surely plays a role.

4. Conclusions

We have shown here a new coating method for lead heritage metal objects. As shown by FT-IR and XRD, a $Pb(C_{14})_2$ coating is formed spontaneously upon immersion of a lead object in a melted sample of tetradecanoic acid at 60 °C, followed by careful rinsing in ethanol. The coating formation method is extremely simple, inexpensive and non-contaminant. The melted tetradecanoic sample can be reused many times. Some traces of corrosion products are observed upon formation of the coating and before exposure of coated samples to corrosive environments. These corrosion products are likely to have been formed upon exposure of the lead sample to 60 °C. Shorter coating formation times (currently 18 hours) might decrease the unwanted corrosion during the coating formation process, while still producing coatings with excellent barrier properties. Work in this direction is ongoing.

Linear Sweep Voltammograms, and time lapse Electrochemical Impedance Spectroscopy and X-Ray diffraction experiments have shown the excellent capabilities of these coatings towards corrosion resistance. The shape and magnitude of the Bode plots was almost unaltered during 53 days of exposure to corrosive media, while XRD patterns remained mostly unchanged during 59 days of exposure to a humid and oak vapour rich atmosphere.

The low cost and simplicity of the coating method makes it an interesting candidate to test its applicability on real heritage objects.

Acknowledgments

This work was funded by a Marie Curie IntraEuropean Fellowship (Pbcoatings). Pricreator Renaissance Products, UK, is acknowledge for the generous free sample of the micro-crystalline wax pollish.

Appendix A. Supplementary data

Supplementary data associated with this article can be found, in the online version, at http://dx.doi.org/10.1016/j.electacta.2015.05.022.

References

[1] A. Adriaens, M. Dowsett, The coordinated use of synchrotron spectroelectrochemistry for corrosion studies on heritage metals, Acc. Chem. Res. 43 (2010) 927.
[2] E. Cano, D. Lafuente, D.M. Bastidas, Use of EIS for the evaluation of the protective properties of coatings for metallic cultural heritage: A review, J. Solid State Electrochem. 14 (2010) 381.
[3] M. Dowsett, A. Adriaens, B. Schotte, G. Jones, L. Bouchenoire, In-situ spectroelectrochemical study of the growth process of a lead decanoate coating as corrosion inhibitor for lead surfaces, Surf. Interface Anal. 41 (2009) 565.
[4] V. Costa, F. Urban, Lead and its alloys: metallurgy, deterioration and conservation, Reviews in Conservation 6 (2005) 52.
[5] T.E. Graedel, Chemical mechanisms for the atmospheric corrosion of lead, J. Electrochem. Soc. 141 (1994) 922.
[6] A. Niklasson, L.G. Johansson, J.E. Svensson, Influence of acetic acid vapor on the atmospheric corrosion of lead, J. Electrochem. Soc. 152 (2005) B519.
[7] J. Tétreault, J. Sirois, E. Stamatopoulou, Studies of lead corrosion in acetic acid environments, Studies in Conservation 43 (1998) 17.
[8] T. Clarke, Organ failure, Nature 427 (2004) 8.
[9] B. Schotte, A. Adriaens, Treatments of corroded lead artefacts: An overview, Studies in Conservation 51 (2006) 297.
[10] R. Grayburn, M. Dowsett, M. De Keersmaecker, E. Westenbrink, J.A. Covington, J.B. Crawford, M. Hand, D. Walker, P.A. Thomas, D. Banerjee, A. Adriaens, Time-lapse synchrotron X-ray diffraction to monitor conservation coatings for heritage lead in atmospheres polluted with oak-emitted volatile organic compounds, Corrosion Science 82 (2014) 280.
[11] C. Chiavari, C. Martini, D. Prandstraller, A. Niklasson, L.-G. Johansson, J.-E. Svensson, A. Aslund, C.J. Bergsten, Atmospheric corrosion of historical organ pipes: The influence of environment and materials, Corrosion Science 50 (2008) 2444.
[12] E. Rocca, C. Rapin, F. Mirambet, Inhibition treatment of the corrosion of lead artefacts in atmospheric conditions and by acetic acid vapour: Use of sodium decanoate, Corrosion Science 46 (2004) 653.
[13] E. Rocca, J. Steinmetz, Inhibition of lead corrosion with saturated linear aliphatic chain monocarboxylates of sodium, Corrosion Science 43 (2001) 891.
[14] M. De Keersmaecker, K. De Wael, A. Adriaens, The use of lead dodecanoate as an environmentally friendly coating to inhibit the corrosion of lead objects: Comparison of three different deposition methods, Progress in Organic Coatings 74 (2012) 1.
[15] M. De Keersmaecker, K. De Wael, A. Adriaens, Influence of the deposition method, temperature and deposition time on the corrosion inhibition of lead dodecanoate coatings deposited on lead surfaces, Journal of Solid State Electrochemistry 17 (2013) 1259.
[16] M. De Keersmaecker, D. Depl, K. Verbeken, A. Adriaensa, Electrochemical and surface study of neutralized dodecanoic acid on a lead substrate, Journal of the Electrochemical Society 161 (2014) C126.
[17] M. De Keersmaecker, M. Dowsett, R. Grayburn, D. Banerjee, A. Adriaens, In-situ spectroelectrochemical characterization of the electrochemical growth and breakdown of a lead dodecanoate coating on a lead substrate, Talanta 132 (2015) 760.
[18] M. De Keersmaecker, K. Verbeken, A. Adriaens, Lead dodecanoate coatings for the protection of lead and lead-tin alloy artifacts: Two examples, Applied Surface Science 292 (2014) 149.
[19] K. De Wael, M. De Keersmaecker, M. Dowsett, D. Walker, P.A. Thomas, A. Adriaens, Electrochemical deposition of dodecanoate on lead in view of an environmentally safe corrosion inhibition, Journal of Solid State Electrochemistry 14 (2010) 407.
[20] R. Grayburn, M. Dowsett, M. De Keersmaecker, D. Banerjee, S. Brown, A. Adriaens, Towards a new method for coating heritage lead, Heritage Science 2 (2014) 14.
[21] A. Adriaens, M. Dowsett, K. Leyssens, B. Van Gasse, Insights into electrolytic stabilization with weak polarization as treatment for archaeological copper objects, Anal. Bioanal. Chem. 387 (2007) .
[22] M.A. Mesubi, An infrared study of zinc, cadmium, and lead salts of some fatty acids, Journal of Molecular Structure 81 (1982) 61.
[23] N.W. Alcock, V.M. Tracy, T.C. Waddington, Acetates and acetato-complexes. Part 2. Spectroscopic studies, Journal of the Chemical Society, Dalton Transactions (1976) 2243.
[24] F. Lacouture, M. François, C. Didierjean, J.-P. Rivera, E. Rocca, J. Steinmetz, Anhydrous lead(II) heptanoate, Acta Cryst. C 57 (2001) 530.
[25] A. Lasia, Electrochemical Impedance Spectroscopy and its Applications, Springer, 2014.
[26] M.E. Orazem, B. Tribollet, Electrochemical impedance spectroscopy, John Wiley & Sons, 2008.
[27] A. Amirudin, D. Thieny, Application of electrochemical impedance spectroscopy to study the degradation of polymer-coated metals, Progress in Organic Coatings 26 (1995) 1.
[28] G.J. Brug, A.L.G.v.d. Eeden, M. Sluyters-Rehbach, J.H. Sluyters, The analysis of electrode impedances complicated by the presence of a constant phase element, J. Electroanal. Chem. 176 (1984) 275.
[29] J.C. Galván, S. Feliu, M. Morcillo, Reproducibility of electrical impedance data for a metal/paint system, Progress in Organic Coatings 17 (1989) 135.